Molecular Gas Dynamics Approaches to Interfacial Phenomena Accompanied with Condensation

S. Mikami, K. Kobayashi, T. Ota, S. Fujikawa, T. Yano, M. Ichijo

Division of Mechanical and Space Engineering, Graduate School of Engineering, Hokkaido University, Sapporo, 060-8628, Japan

Abstract

This paper deals with the condensation coefficient of methanol, which is evaluated from a condensation rate at the vapor-liquid interface. Film condensation is induced on the endwall of a vapor-filled shock tube, when a shock wave is reflected at the endwall and the vapor becomes supersaturated there. The liquid film grows with the lapse of time. The evolution in time of the liquid film thickness is measured by an optical interferometer with a high accuracy, and thereby the net condensation mass flux at the interface is obtained. The mass flux is incorporated into the kinetic boundary condition (KBC) at the interface for the Gaussian-BGK Boltzmann equation. Such a treatment of the boundary condition makes it possible to formally eliminate the evaporation and condensation coefficients in KBC and to obtain the unique numerical solution of the vapor-liquid system. In this way, the instantaneous condensation coefficient is accurately evaluated from the conformity with experiment and numerical solution. It is found that the values of condensation coefficient are, near vapor-liquid equilibrium states, close to those evaluated by molecular dynamics simulations.

Preprint submitted to Elsevier Science *1 November 2006*

Key words: condensation; kinetic boundary condition; condensation coefficient; molecular gas dynamics; shock tube

Nomenclature

Principal symbols

f	velocity distribution function [$\mathrm{s^3 m^{-6} J^{-n/2} kg^{1+n/2}}$]
M_s	Mach number of incident shock wave [−]
n	internal degree of freedom [−]
p	pressure [Pa]
R	gas constant [$\mathrm{J\ kg^{-1} K^{-1}}$]
t	time [s]
T	temperature [K]
v	velocity [$\mathrm{m\ s^{-1}}$]
α_c	condensation coefficient [−]
α_e	evaporation coefficient [−]
γ	specific heats ratio [−]
η	internal energy parameter [$\mathrm{J^{n/2} kg^{-n/2}}$]
ξ	molecular velocity [$\mathrm{m\ s^{-1}}$]
ρ	density [$\mathrm{kg\ m^{-3}}$]

Email address: fujikawa@eng.hokudai.ac.jp (S. Mikami, K. Kobayashi, T. Ota, S. Fujikawa, T. Yano, M. Ichijo).

Subscripts and superscript

b	behind incident shock wave
ℓ	liquid film
x	x-component
y	y-component
z	z-component
$*$	saturated value
0	initial value

1 Introduction

The evaporation and condensation process at a vapor-liquid interface is a fundamental subject relating to various fields in engineering as well as physics, chemistry, meteorology. One of unresolved problems is the kinetic boundary condition (KBC) at the vapor-liquid interface, which has relevance to drag and lift on the body and heat and mass transfer across the boundary. While the governing equations (the Navier-Stokes equations in fluid dynamics and the Boltzmann equation in molecular gas dynamics) can be derived from macroscopic or microscopic conservation laws, the derivation of KBC requires detailed information of the interface in molecular scales.

Previous investigations of boundary conditions at the interface can be classified into two categories. One is the analytical derivation of boundary conditions used with the Navier-Stokes equations [1]. Here, the Boltzmann equation has been applied to derive fluid dynamic boundary conditions on the velocity and temperature of the vapor at the interface. However, the physically correct form of KBC has been unknown, and the only model has been used up to now [1,2]. The other is the formulation of a physically grounded KBC by

molecular dynamics which can provide further detailed information of molecular phenomena at the interface. Ishiyama et al. [3–6] have elucidated that the conventional KBC used in molecular gas dynamics is valid at a rather low temperature and weak condensation state. Here, we shall remark that the KBC includes two parameters. These parameters are called condensation coefficient α_c and evaporation coefficient α_e. Condensation and evaporation coefficients are defined, respectively, as the ratio of the condensed flux to the vapor flux colliding onto the interface and the ratio of the spontaneously evaporating flux from the interface to the flux outgoing from it in an equilibrium state. Historically, values of these coefficients, e.g., for water, has excited much controversy [7]. Ishiyama et al. have determined these coefficients of argon in equilibrium and nonequilibrium states [3,6] and evaporation coefficients of methanol and water in equilibrium states [4,5].

On the other hand, Fujikawa et al. [8] have proposed a method for the determination of condensation coefficient by combining an experiment of film condensation of a vapor on the endwall of a shock tube and the corresponding numerical analysis of the Navier-Stokes equation with the fluid dynamic boundary conditions on the velocity and temperature of the vapor at the interface derived by Sone and Onishi [9] from the asymptotic analysis of the Boltzmann equation. A thin liquid film is formed on the endwall and it grows with the lapse of time after a shock wave in the vapor is reflected there. The evolution in time of the liquid film thickness is measured by an optical interferometer. The liquid film thickness is compared with the counterpart obtained by the numerical analysis with provisional values of condensation coefficient α included in the boundary conditions (only one parameter α has been considered as $\alpha_c = \alpha_e$ in Ref. [8]). The process of the comparison is repeated by

changing the provisional values until the difference between the experimental and numerical results becomes sufficiently small, and thus we can determine the most probable value of condensation coefficient α for each experimental condition. Recently, we have improved the numerical analysis by adopting the polyatomic version of Gaussian-BGK Boltzmann equation [10]. It enables us to eliminate some assumptions prerequisite for the method in Ref. [8]: (i) steady, (ii) weak condensation and (iii) monatomic molecules [11]. Furthermore, by using the net condensation mass flux obtained from the experiment, the method which can accurately evaluate the instantaneous condensation coefficient have been formulated [12].

As discussed previously, the problem of KBC and condensation and evaporation coefficients is significantly important and further study based on molecular gas dynamics approaches can resolve it. Accordingly, the authors undertook the investigation reported here.

2 Problem statement

Figure 1 shows the propagation process of a shock wave in a vapor advancing toward and reflecting from the endwall of a shock tube. Just at the instant when the shock wave is reflected at the endwall on which an adsorbed liquid film with a thickness of a molecular scale initially exists, the pressure, temperature, and density of the vapor increase in a stepwise fashion far from the endwall and these are held at higher values compared with the initial ones. However, the vapor temperature adjacent to the endwall increases little because the endwall made of a thick glass has a sufficiently large heat capacity compared with the vapor, whereas the vapor pressure is almost uniform be-

tween the reflected shock wave and the endwall. Thus, the vapor becomes supersaturated on the initially adsorbed liquid film and condenses in the form of a liquid film.

Behind the reflected shock wave, the vapor flow toward the interface is induced due to condensation. The liquid film grows with the lapse of time. Such a condensation phenomenon provides us an ideal situation to which molecular gas dynamics can be applied. It is also expected that the analysis based on molecular gas dynamics for the propagation process of the shock wave accompanied with condensation will be of intrinsic interest, because it deals with molecular phenomena of one-dimensional heat and mass transfer at the vapor-liquid interface.

3 Methods

3.1 Experimental setup

Figure 2 shows a horizontal type of shock tube used in the experiment. The length of the low pressure section (the test section) is 2830 mm, while the length of the high pressure section is 2600 mm. These sections are divided by a thin aluminum diaphragm. The cross section of the tube is the circle of 74.3 mm in diameter. The endwall of the low pressure section consists of a quartz glass with the thickness of 15 mm, the inner surface of which is polished at the flatness level of $\lambda/20$ ($\lambda = 632.8$nm) to prevent the diffused reflection of a laser beam for optical measurement and to make the laser–shed region of a liquid film on the surface as uniform as possible. The attained vacuum level of the test section is 1.5×10^{-3} Pa, and the final pressure of noncondensable

gases may be about 0.05 Pa, just before an experiment run, due to a slight leakage of outside gases into the tube. However, it is clarified in Ref. [13] that the noncondensable gases have no influence at all on the growth of liquid film in conditions of the present experiment.

Methanol vapor is used as the test gas because of the easiness of treatment; it has a rather high saturated vapor pressure at a room temperature. Concerning the molecular association of the vapor, the degree of association is estimated to be 0.16 % at 290 K and 2 kPa, so that it is negligible [14]. Before the start of each experiment, the initial pressure of the test vapor is measured by a pressure gauge (type 122A, MKS Instruments Inc., Andover, MA, USA) and initial temperatures of the vapor and the endwall are measured by thermocouples. The nitrogen gas, driver gas, is introduced into the high pressure section, and the diaphragm is naturally ruptured by a pressure difference between the driver gas and the test vapor. Then a shock wave is generated and propagates toward the endwall in the low pressure section. The Mach number of incident shock wave is evaluated from the distance (=1000 mm) between two pressure gauges (type 701A, Kistler Instrument AG, Winterthur, Switzerland) and the passage time of the shock wave between them, and the vapor pressures behind the incident and reflected shock waves are measured by the pressure gauge.

The variation in time of a liquid film thickness is obtained by the measurement of the light reflectance from the optically transparent film system, because the growing film, together with the glass endwall, forms a kind of interferometer. All data except for the temperatures are recorded in digital storage oscilloscopes and then processed by a computer. In the previous experiments [13,15], the time interval of data acquisition in the reflectance was 1-2 μs, whereas the interval is 2 ns in the present experiment. Thus, the accuracy of the measure-

ment of liquid film thickness is greatly enhanced. All experiments are carried out at room temperatures (295-300 K).

3.2 Theoretical

The numerical analysis based on molecular gas dynamics is done for the problem mentioned in Sec. 2. As shown in Fig. 3, a steady shock wave with plane front is formed far from the endwall and propagates toward it. An adsorbed liquid film is supposed to exist initially on the endwall, as it does actually [15]. After the shock wave is reflected at the endwall, condensation takes place filmwise on the surface of initially adsorbed liquid film, and the liquid film grows with the lapse of time. The temperatures of liquid film and endwall change due to the release of latent heat of condensation. Therefore, we need to solve the Gaussian-BGK Boltzmann equation for the vapor together with the heat conduction equations for the liquid film and endwall.

The following assumptions are made: (i) the vapor flow is one-dimensional, (ii) the initial temperatures of vapor, liquid film, and endwall are equal, (iii) in front of the incident shock wave with Mach number M_s, the distribution function of vapor molecules is a stationary Maxwellian with the temperature T_0 and the density ρ_0, (iv) behind the shock wave, the distribution function of vapor molecules is also Maxwellian with T_b, ρ_b and velocity v_b. The quantities in front of and behind the shock wave are connected by Rankine-Hugoniot relations. The coordinate x is originated from the interface of the endwall and directed toward the vapor phase. The Gaussian-BGK Boltzmann equation are solved with the following KBC for outgoing molecules from the interface [16]:

$$f^{\text{out}} = [\alpha_e \rho^* + (1-\alpha_c)\sigma] a_M b_M, \quad (\xi_x > v_\ell), \tag{1}$$

$$a_M = \frac{1}{(2\pi R T_\ell)^{3/2}} \exp\left(-\frac{(\xi_x - v_\ell)^2 + \xi_y^2 + \xi_z^2}{2RT_\ell}\right), \tag{2}$$

$$b_M = \frac{1}{\Gamma(\frac{n}{2}+1)(RT_\ell)^{n/2}} \exp\left(-\frac{\eta^{2/n}}{RT_\ell}\right), \tag{3}$$

where α_e is evaporation coefficient, α_c condensation coefficient, ρ^* the saturated vapor density at the surface temperature of liquid film T_ℓ, ξ the molecular velocity with components (ξ_x, ξ_y, ξ_z), and v_ℓ the moving velocity of the vapor-liquid interface, i.e. the liquid film surface by condensation, Γ the gamma function, η the internal energy parameter, n the internal degree of freedom of a vapor molecule; it is taken to be 6 so that the theoretical value ($\gamma = 1.222$) of specific heats ratio may coincide well with the experimental one ($\gamma = 1.228$). The symbol σ is defined by

$$\sigma = -\sqrt{\frac{2\pi}{RT_\ell}} \int_{\xi_x < v_\ell} (\xi_x - v_\ell) f^{\text{coll}} \mathrm{d}\xi_x \mathrm{d}\xi_y \mathrm{d}\xi_z \mathrm{d}\eta, \tag{4}$$

where R is the gas constant of the vapor, f^{coll} the distribution function of molecules incident on the interface. The triple integral with respect to ξ_i ($i = x, y, z$) is carried out over the whole space of ξ_i unless otherwise stated, and the integral with respect to η is carried out in a half space $[0, \infty)$.

In this study, we use the numerical method proposed in recent studies [11,12]. The method focuses on the net mass flux across the interface. The flux $\rho_\ell v_\ell$ can be written as

$$\rho_\ell v_\ell = (\alpha_c \sigma - \alpha_e \rho^*) \sqrt{\frac{RT_\ell}{2\pi}}, \tag{5}$$

where ρ_ℓ is the density of liquid film. Making use of Eq. (5) allows to eliminate

α_c and α_e from Eq. (1) and leads to

$$f^{\rm out} = \left(\sigma - \rho_\ell v_\ell \sqrt{\frac{2\pi}{RT_\ell}}\right) a_M b_M, \quad (\xi_x > v_\ell). \tag{6}$$

Therefore, once v_ℓ is experimentally given as a function of time, the Gaussian BGK-Boltzmann equation can be solved with the distribution function $f^{\rm out}$. In consequence, $\rho_\ell v_\ell$, T_ℓ, ρ^* and σ of Eq. (5) become known, and the unknowns are α_c and α_e. Note that α_e is, from the definition, a function of T_ℓ [3]. Therefore condensation coefficient α_c can be evaluated from Eq. (5) by using the value of evaporation coefficient, $\alpha_e = 0.86$ estimated in Refs. [4,5].

4 Results

Figure 4 shows a typical example of time history of the light reflectance measured by the optical interferometer with high response performance. The dashed line denotes the average value for the time before condensation onset. Before the onset, the surface of initially adsorbed liquid film can be considered to remain unchanged. By condensation, the reflectance changes in proportion to the time for 0.3-0.4 μs. The change in reflectance during this time is well approximated by a solid straight line determined by the least square method. The onset time is defined as the intersecting point of the solid and dashed lines.

Figure 5 shows the variation in time of the liquid film thickness obtained by converting the data of Fig. 4 with the optical theory [13]. The abscissa is the time, whose origin is the onset time of condensation, and the ordinate is the liquid film thickness. The closed circles denote the converted data, and a straight solid line is an approximate curve for them. The slope of the curve

means the moving velocity of the vapor-liquid interface v_ℓ. It is found that the curve can be approximated well by the straight line, i.e. v_ℓ=constant for a short time. It is also confirmed that the almost the same slope can be obtained if the initial conditions (p_0, T_0 and M_s) are almost the same.

Figure 6 shows variations in time of fluid dynamical quantities at the vapor-liquid interface. The abscissa is the time and the origin is the onset time of condensation. After the onset time, the shock wave still continues interacting at the liquid film surface and the vapor temperature T, pressure p, and σ increase rapidly after the condensation took place. These quantities set in an almost steady state immediately. Then, from Fig. 6 (a), one can see that the variation in the liquid film temperature T_ℓ is less than 1%. Therefore those of saturated vapor pressure p^* and density ρ^* are less than 10%. As a result, from Eq. (5), α_c is regarded as a constant value for a short time interval 0.03-0.2 μs after the condensation onset.

Figure 7 shows the relationship between condensation coefficient and the ratio of the vapor pressure to the saturated vapor pressure at the vapor-liquid interface for ten experimental data shown in Table 1. The abscissa is the pressure ratio p/p^*, and the ordinate is condensation coefficient. These are values at 0.2 μs after the condensation onset. The vapor-liquid system is in an equilibrium state in the case where p/p^* is unity: $\rho_\ell v_\ell = 0$ and $\alpha_c = \alpha_e$. The dashed line denotes the value of evaporation coefficient obtained from the molecular dynamics simulations [4,5]. The values of condensation coefficient are found to be from 0.8 to 0.9, and these are close to the ones of evaporation coefficient.

5 Conclusion

The condensation coefficient of methanol has been determined by the improved molecular gas dynamics method. The moving velocity of vapor-liquid interface, obtained from the measurement of liquid film thickness, has been incorporated into KBC and it has been used for solving the Gaussian BGK-Boltzmann equation. The results have shown that the condensation coefficient of methanol takes values from 0.8 to 0.9 near vapor-liquid equilibrium states at T_ℓ = 295-300(K), which are close to the values of evaporation coefficient (condensation coefficient at equilibrium states) evaluated in recent molecular dynamics simulations [4,5].

References

[1] Y. Sone, Kinetic Theory and Fluid Dynamics, Birkhäuser, Boston, 2002.

[2] C. Cercignani, Rarefied Gas Dynamics: From Basic Concepts to Actual Calculations, Cambridge University Press, New York, 2000.

[3] T. Ishiyama, T. Yano, S. Fujikawa, Molecular dynamics study of kinetic boundary condition at an interface between argon vapor and its condensed phase, Phys. Fluids **16** (8) (2004) 2899-2906.

[4] T. Ishiyama, T. Yano, S. Fujikawa, Molecular dynamics study of kinetic boundary condition at an interface between a polyatomic vapor and its condensed phase, Phys. Fluids **16** (12) (2004) 4713-4726.

[5] T. Ishiyama, T. Yano, S. Fujikawa, Molecular dynamics study on the evaporation part of the kinetic boundary condition at the interface between water and water vapor, AIP Conference Proc. **762** (1) (2005) 491-496.

[6] T. Ishiyama, T. Yano, S. Fujikawa, Kinetic boundary condition at a vapor-liquid interface, Phys. Rev. Lett. **95** (2005) 084504.

[7] R. Marek, J. Straub, Analysis of the evaporation coefficient and the condensation coefficient of water, J. Heat Mass Transf. **44** (2001) 39-53.

[8] S. Fujikawa, M. Okuda, T. Akamatsu, T. Goto, Non-equilibrium vapour condensation on a shock-tube endwall behind a reflected shock wave, J. Fluid Mech. **183** (1987) 293-324.

[9] Y. Sone, Y. Onishi, Kinetic theory of evaporation and condensation: hydrodynamic equations and slip boundary conditions, J. Phys. Soc. Japan **44** (1978) 1981-1994.

[10] P. Andries, P. Le Tallec, J. P. Perlat, B. Perthame, The Gaussian-BGK model of Boltzmann equation with small Prandtl number, Eur. J. Mech. B-Fluids **19** (2000) 813-830.

[11] T. Yano, K. Kobayashi, S. Fujikawa, Numerical study of condensation of a polyatomic vapor by a shock wave based on the kinetic theory of gases, in: Proc. JSME-ASME Fluids Engineering Division Summer Meeting, Honolulu, America, 6-10 July, 2003, FEDSM 2003-45022.

[12] K. Kobayashi, S. Fujikawa, T. Yano, A new approach for determination of condensation coefficient of methanol by combining molecular gas dynamics study and shock tube experiment, in: Proc. 6th World Conference on Experimental Heat Transfer, Fluid Mechanics and Thermodynamics, Matsushima, Japan, 17-21 April, 2005, 7-b-7.

[13] M. Maerefat, S. Fujikawa, T. Akamatsu, Non-equilibrium condensation of a vapour-gas mixture on a shock-tube endwall behind a reflected shock wave, Fluid Dyn. Res. **6** (1990) 25-42.

[14] S. Fujikawa, T. Yano, K. Kobayashi, K. Iwanami, M. Ichijo, Molecular gas dynamics applied to phase change processes at a vapor-liquid interface: shock-tube experiment and MGD computation for methanol, Exps. Fluids **37** (2004) 80-86.

[15] M. Maerefat, T. Akamatsu, S. Fujikawa, Non-equilibrium condensation of water and carbon tetrachloride vapour in a shock-tube, Exps. Fluids **9** (1990) 345-351.

[16] C. Cercignani, W. Fiszdon, A. Frezzotti, The paradox of the inverted temperature profiles between an evaporating and a condensing surface, Phys. Fluids **28** (1985) 3237-3240.

Figure legends

Fig. 1 : The growth of a liquid film on shock tube endwall behind a reflected shock wave in a vapor.

Fig. 2 : The schematic diagram of experimental setup.

Fig. 3 : The schematic diagram of model.

Fig. 4 : The measured intensity of light reflectance converted into voltage: Condition No. 10 in Table 1.

Fig. 5 : The liquid film thickness obtained from the data of Fig 4.

Fig. 6 : The variations in time of fluid-dynamical quantities at the vapor-liquid interface. The condition is the same as in Figs. 4 and 5.

Fig. 7 : The pressure ratio p/p^* dependency of condensation coefficient.

Table 1

The experimental data: p_0 and T_0 are initial pressure and initial temperature of methanol vapor, M_s is Mach number of incident shock wave.

No.	T_0 [K]	p_0 [Pa]	M_s
1	296.65	1999.8	1.73
2	297.45	1999.8	1.75
3	295.55	1999.8	1.74
4	298.35	3002.4	1.62
5	299.65	4002.3	1.54
6	296.05	2013.2	1.73
7	295.15	2098.5	1.72
8	298.45	4066.3	1.54
9	297.95	3999.7	1.53
10	298.35	3994.3	1.55

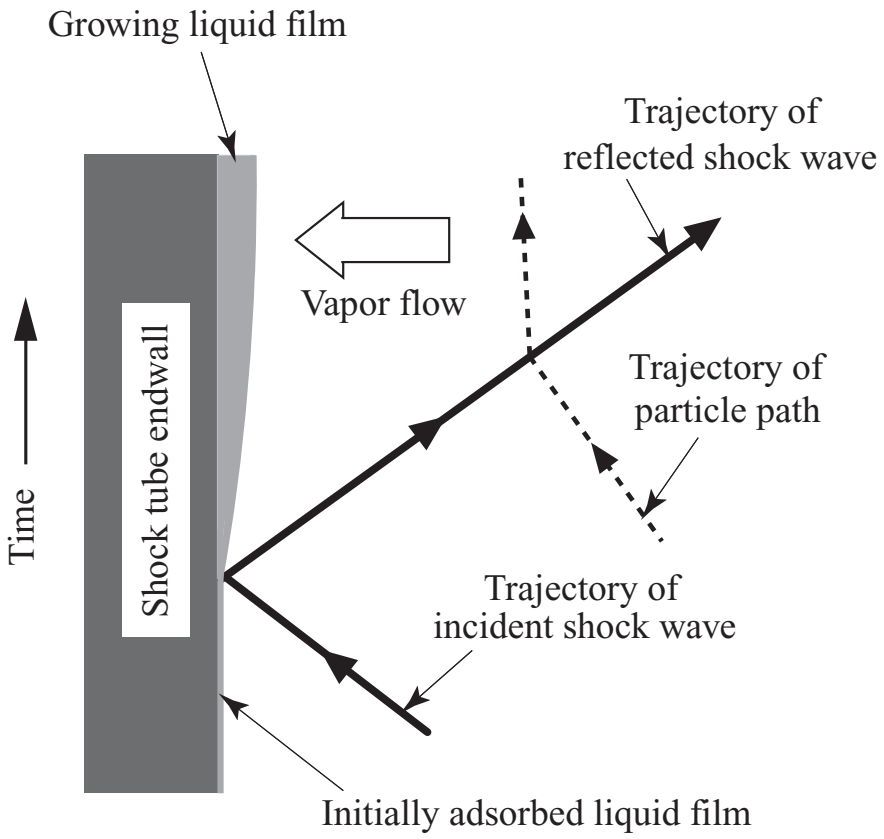

Fig. 1. The growth of a liquid film on shock tube endwall behind a reflected shock wave in a vapor.

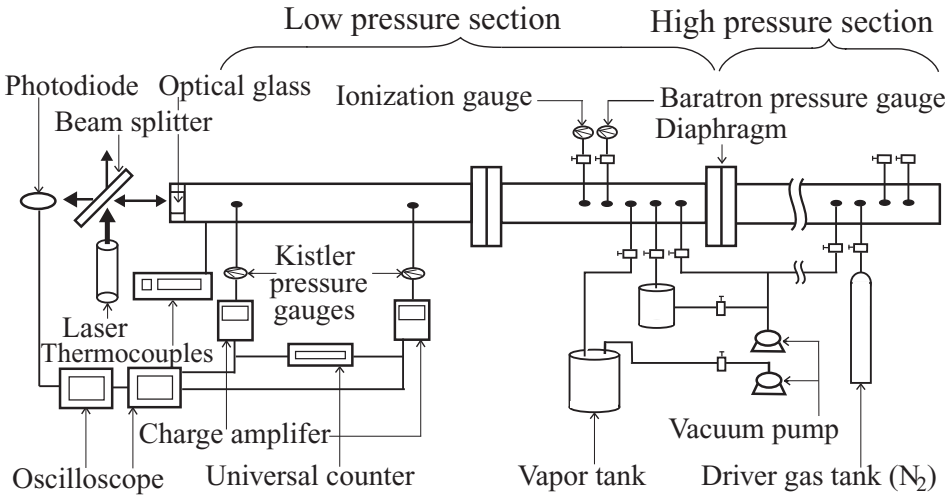

Fig. 2. The schematic diagram of experimental setup.

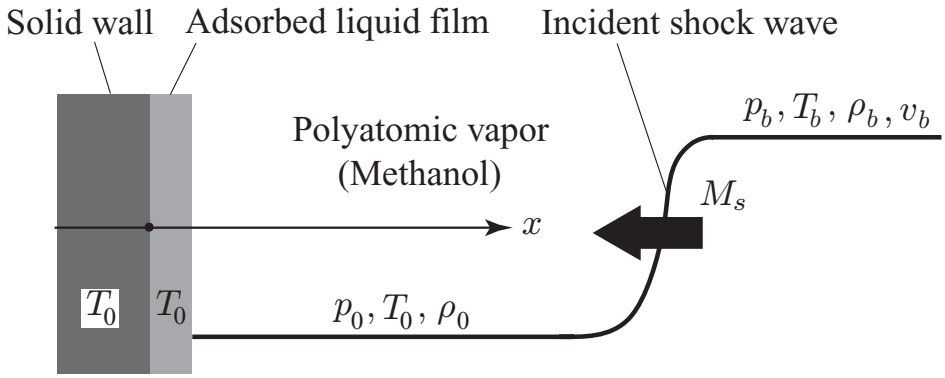

Fig. 3. The schematic diagram of model.

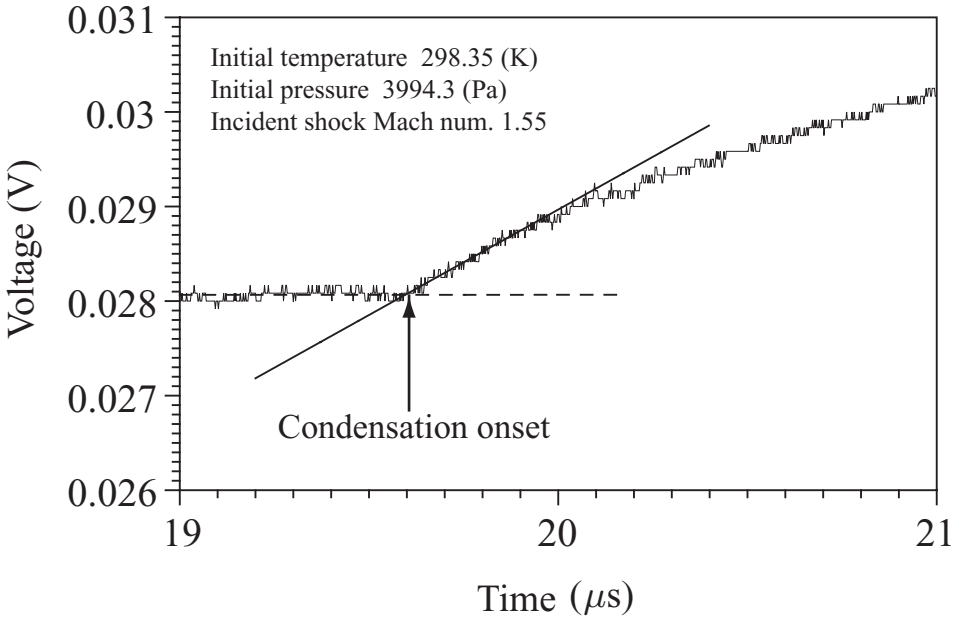

Fig. 4. The measured intensity of light reflectance converted into voltage: Condition No. 10 in Table 1.

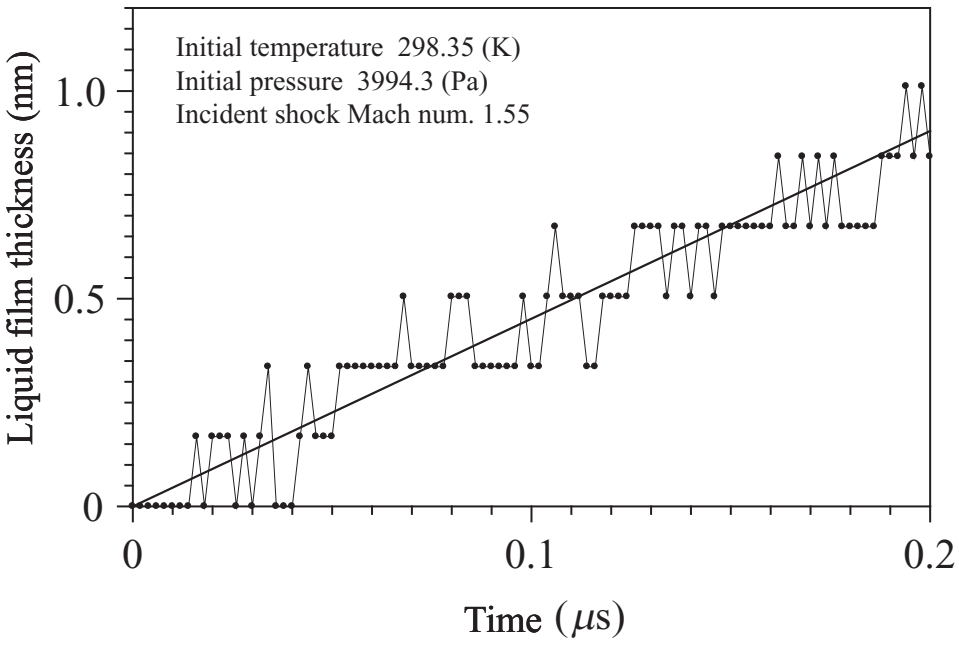

Fig. 5. The liquid film thickness obtained from the data of Fig 4.

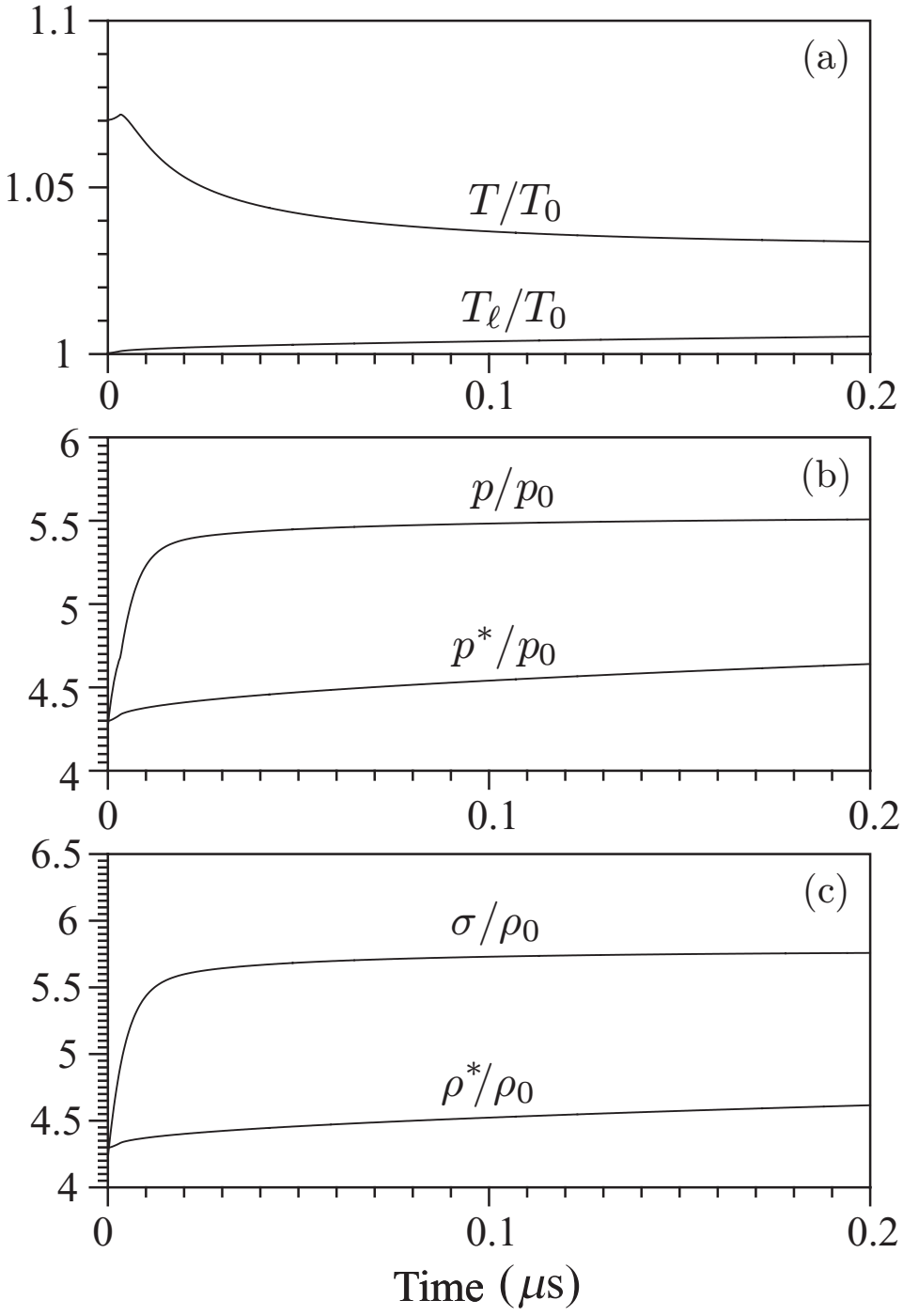

Fig. 6. The variations in time of fluid-dynamical quantities at the vapor-liquid interface. The condition is the same as in Figs. 4 and 5.

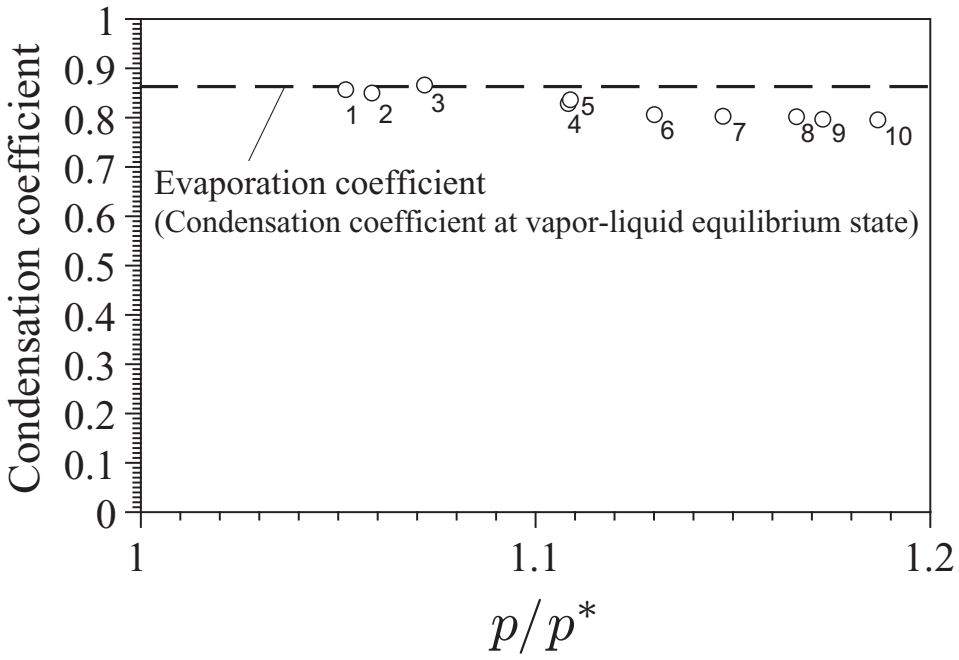

Fig. 7. The pressure ratio p/p^* dependency of condensation coefficient.